Fluorescence-microscopy-based assay assessing regulatory mechanisms of global genome nucleotide excision repair in cultured cells

Kusakabe, Masayuki

Sugasawa, Kaoru

(Citation)
STAR Protocols,4(3):102378

(Issue Date)
2023-09-15

(Resource Type)
journal article

(Version)
Version of Record

STAR Protocols

CellPress
OPEN ACCESS

Protocol

Fluorescence-microscopy-based assay assessing regulatory mechanisms of global genome nucleotide excision repair in cultured cells

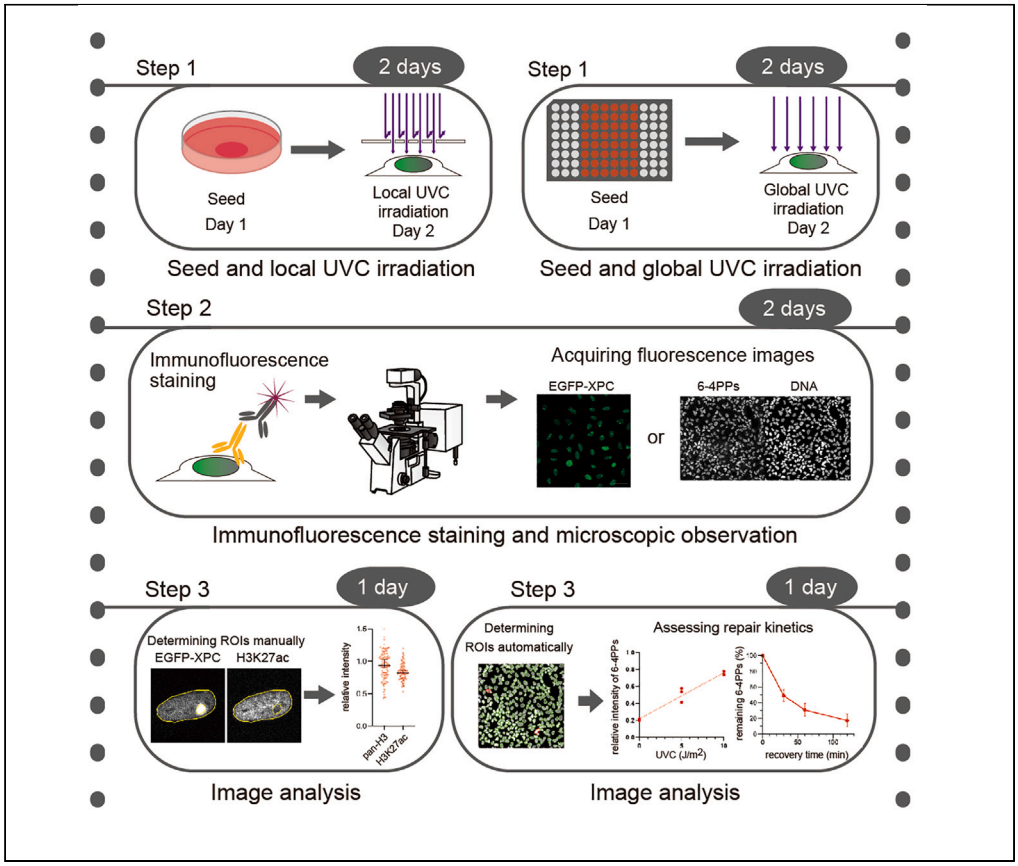

It remains uncertain how global genome nucleotide excision repair (GG-NER) efficiently removes various helix distorting DNA lesions in the cell nucleus. Here, we present a protocol to assess the contribution of factors of interest to GG-NER using two types of fluorescence-microscopy-based techniques. First, we describe steps for analyzing the localization of the factors upon local ultraviolet (UV) irradiation. We then detail the second technique, which quantifies the removal of UV-induced photolesions combined with lesion-specific antibodies and program-based image analysis.

Publisher's note: Undertaking any experimental protocol requires adherence to local institutional guidelines for laboratory safety and ethics.

Masayuki Kusakabe, Kaoru Sugasawa

ksugasawa@garnet.kobe-u.ac.jp

Highlights

Two fluorescence-microscopy-based protocols for assessing progression of GG-NER

Evaluating localization of factors of interest by local UV irradiation

Visualizing UV-induced photolesions with lesion-specific antibodies

Program-based image analysis enabling assessment of repair kinetics of GG-NER

Kusakabe & Sugasawa, STAR Protocols 4, 102378 September 15, 2023
https://doi.org/10.1016/j.xpro.2023.102378

STAR Protocols

CellPress
OPEN ACCESS

Protocol

Fluorescence-microscopy-based assay assessing regulatory mechanisms of global genome nucleotide excision repair in cultured cells

Masayuki Kusakabe[1,2] and Kaoru Sugasawa[1,3,*]

[1]Biosignal Research Center and Graduate School of Science, Kobe University, Kobe 657-8501, Japan

[2]Technical contact: mkusakabe@people.kobe-u.ac.jp

[3]Lead contact

*Correspondence: ksugasawa@garnet.kobe-u.ac.jp
https://doi.org/10.1016/j.xpro.2023.102378

SUMMARY

It remains uncertain how global genome nucleotide excision repair (GG-NER) efficiently removes various helix distorting DNA lesions in the cell nucleus. Here, we present a protocol to assess the contribution of factors of interest to GG-NER using two types of fluorescence-microscopy-based techniques. First, we describe steps for analyzing the localization of the factors upon local ultraviolet (UV) irradiation. We then detail the second technique, which quantifies the removal of UV-induced photolesions combined with lesion-specific antibodies and program-based image analysis.

For complete details on the use and execution of this protocol, please refer to Kusakabe et al.[1]

BEFORE YOU BEGIN

Nucleotide excision repair (NER) is a DNA repair pathway that removes various helix-distorting DNA lesions, including DNA photolesions induced by UV, such as cyclobutane pyrimidine dimers (CPDs) and pyrimidine (6–4) pyrimidone photoproducts (6-4PPs), and bulky base adducts induced by numerous carcinogens.[2] In humans, hereditary defects in NER are implicated in several autosomal recessive disorders, such as xeroderma pigmentosum (XP). Eukaryotic NER consists of two damage recognition sub-pathways: global genome NER (GG-NER), which can eliminate lesions from the whole genome, and transcription-coupled NER (TC-NER), which specifically removes lesions from actively transcribed DNA strands. In mammalian GG-NER, a DNA-binding protein complex containing one of the XP-related gene products, XPC (XPC-RAD23-CETN2 heterotrimer), plays a key role in the recognition of DNA lesions and initiates GG-NER.[3,4] Although multiple factors have been suggested to support the damage recognition by XPC *in vivo*, such as UV-damaged DNA-binding protein (UV-DDB) consisting of DDB1 and DDB2 (XPE) subunits, it remains elusive how XPC efficiently detects DNA lesions in cell nucleus.

To examine the mechanism and regulation of NER and other cellular responses to UV-induced DNA damage, local UV irradiation techniques have made a crucial contribution. Particularly, UV irradiation through isopore membrane filters is a simple and inexpensive method, which has been widely used to elucidate the order of NER factors functioning during the repair process[4,5] and to demonstrate the recruitment of various nuclear factors to UV-damaged chromatin, such as HIRA, CAF-1, and FACT.[6,7] Our recent studies also took advantage of this technique and proposed that histone deacetylation is introduced at DNA damage sites and supports damage recognition by XPC.[1,8] To allow statistical evaluation of the results from the subnuclear DNA damaging experiments in our studies, it was crucial to quantitatively measure fluorescence signals (either fluorescent protein tag or immunofluorescence) at local UV damage (LUD) sites for various chromatin-related protein

factors and/or histone modifications. Herewith we describe our detailed protocols, which are applicable for assessing the localization of various factors upon local UV irradiation in chromatin (we also utilize laser-based local UV stimulation based on three-photon absorption,[9,10] which is not included because it requires a customized, expensive equipment and is not widely available). In addition, we also describe a method, which allows quantitative evaluation of the kinetics of DNA lesion removal in cultured cells, based on global UV irradiation of cells followed by immunofluorescence staining with lesion-specific antibodies. These methods would be widely applicable for analyzing the mechanism and regulation of GG-NER in cultured cells.

Institutional permissions

Usage of recombinant retrovirus was permitted by Kobe University Recombinant DNA Experiments Safety Committee.

Preparation of recombinant retroviruses

Timing: 9–11 days

1. Culture 293-GPG retrovirus packaging cells in a 60 mm dish with the medium specified as '293-GPG maintaining medium'.[11]
2. At 30%–40% confluency, transfect the cells with 6 μg of pMMP-puro retroviral expression vector encoding EGFP-XPC using the FuGENE HD reagent.
3. The next day, replace the medium with 3 mL of standard growth medium.
4. Continue incubation and change the medium every 2 days. Following each medium change, the harvested culture supernatant, which is expected to contain the recombinant retroviruses, is filtrated through a sterile syringe filter (0.45 μm pore size).

   Note: The filter is connected to a 5 mL disposable syringe. The culture supernatant (~3 mL) is passed through the filter and collected in a sterile 15 mL centrifuge tube (Corning).

5. If the recombinant retrovirus is not used immediately, the viral solution is quickly frozen in liquid nitrogen and stored at −80°C as 1 mL aliquots dispensed into sterile 2.0 mL cryovials (TPP).

   Note: We usually use the recombinant retroviruses harvested at 8 days or later after transfection.

Infection with the recombinant retroviruses and selection of stable transformants

Timing: 2 weeks

6. Culture U2OS cells in a 60 mm dish with the standard growth medium up to 30%–40% confluency.
7. If the recombinant retrovirus is stored at -80°C, thaw a vial of the solution quickly with a 37°C water bath. Dilute the recombinant retrovirus solution five times with the standard growth medium (pre-warmed at 37°C). Then, add polybrene to a final concentration of 8 μg/mL.

   Note: Repeated freezing and thawing of the retrovirus solution should be avoided. For infection of cells in a 60 mm dish, we usually use 0.5 mL of the retrovirus solution, which is mixed with 2 mL of the standard growth medium and 1.25 μL of 16 mg/mL polybrene stock solution in a sterile 15 mL centrifuge tube.

8. Discard the medium of the U2OS cell culture. Replenish the dish with 2.5 mL of the diluted retrovirus solution. Then, incubate the cells for 6 h at 37°C.
9. After removing the virus solution, add the standard growth medium and incubate the cells for 24 h at 37°C.

10. Replace the medium with the standard growth medium containing 1 μg/mL puromycin and continue culture over 1 week.

Note: In the case of U2OS cells, we usually observe that uninfected cells start to die and detach from the dish within 2 days in the presence of 1 μg/mL puromycin, while the concentration may need to be determined experimentally if different cell lines are used. In addition, longer incubation may be required if other antibiotics, such as hygromycin B and G418, are used for selection.

Note: The percentage of surviving cells can vary depending on the titer of the retrovirus solution.

11. After obtaining the surviving transformants, confirm the stable expression of EGFP-XPC by western blot analysis according to the previously described procedure (Figure 1A).[1]

Note: We usually maintain the stable transformants with the standard growth medium containing 1 μg/mL puromycin, because removal of puromycin may lead to gradual reduction in the expression of EGFP-XPC. The stable transformants established in this way grow normally in the presence of 1 μg/mL puromycin.

Note: This procedure can be used to establish stable transformants of various cultured cells other than U2OS, such as XP patient-derived cell lines and mouse embryonic fibroblasts.[1,12]

Alternatives: Other plasmid- or virus-based expression systems are also applicable for establishing cells stably expressing XPC fused to a fluorescent protein.

Confirmation of the functionality of EGFP-XPC by immunofluorescence staining

Timing: 2 days

Here, we describe a method to evaluate the localization of factors of interest at LUD sites. This method consists of the following two procedures: 1) local UVC irradiation through a polycarbonate isopore membrane filter, 2) immunofluorescence microscopy.

12. Trypsinize the surviving cells and measure the cell density with a hemocytometer.
13. Seed 3.0×10^5 cells per 35 mm glass bottom dish (with a 14 mm glass bottom hole). Culture the cells for 16–20 h.

Note: We routinely use poly-D-lysine-coated glass bottom dishes purchased from MatTek, and U2OS cells well adhere to the glass surface. Different treatment of dishes may be necessary if other cell lines are used.

14. For preparing local UVC irradiation (step 16), cut polycarbonate isopore membrane filters (5 μm pore size; Merck) such that their diameter is 1–2 mm smaller than that of a glass bottom hole (14 mm) (Figure 1B).
15. Remove the medium carefully with an aspirator and wash the cells with phosphate-buffered saline (PBS) (Figure 1C).

⚠ CRITICAL: Before irradiating the cells with UVC, we remove almost all PBS from a glass bottom dish. However, to prevent excessive detachment of the cells, it is crucial not to remove the solution thoroughly but to leave a small amount of PBS (approximately 10 μL per 14 mm glass bottom hole) at the edge of the glass bottom hole (Figure 1C).

16. Put the filter in the glass bottom hole and irradiate the cells with UVC at a dose of 100–400 J/m^2 under a germicidal lamp with a peak wavelength of 254 nm (Figure 1C).

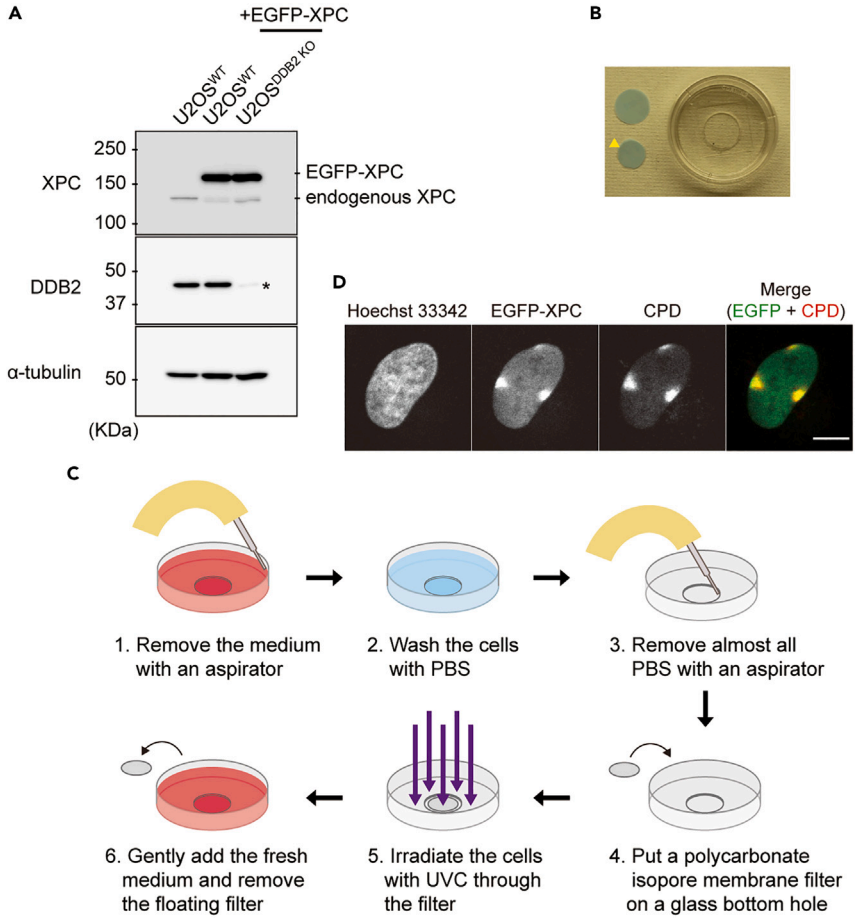

Figure 1. Local UVC irradiation through a polycarbonate isopore membrane filter

(A) Immunoblot analysis confirming the expression of XPC and DDB2 proteins in the cell lines used. For U2OS$^{DDB2\ KO}$ cells, the presence of biallelic mutations of the endogenous *DDB2* gene was confirmed by sequencing; therefore, the faint band marked by an asterisk represents a nonspecific reaction of the antibody used.

(B) A polycarbonate isopore membrane filter was cut such that its diameter was 1–2 mm smaller (yellow arrowhead) than that of a glass bottom hole (14 mm).

(C) Schematic representation of the procedure of UVC irradiation through the filter. The medium was removed with an aspirator, and cells were washed with PBS (1–2). After almost all PBS was removed, the filter was put in the glass bottom hole, and cells were irradiated with UVC (3–5). After gently adding the fresh growth medium, the floating filter was carefully removed (6).

(D) U2OS$^{DDB2\ KO}$ cells stably expressing EGFP-XPC were irradiated with UVC at a dose of 400 J/m^2 through the isopore membrane filter and subjected to immunofluorescence staining after culture for 30 min at 37°C. The localizations of EGFP-XPC and CPDs were visualized by immunofluorescence staining. EGFP and CPDs were visualized with Alexa Fluor 488 and 594, respectively, and nuclear DNA was counterstained with Hoechst 33342. Scale bar: 10 μm.

⚠ CRITICAL: Make sure that the entire surface of the filter is attached to the glass bottom intimately without any flexure. Once the edge of the filter touches the glass bottom, do not lift it up again, as this causes detachment of cells adhered to the filter.

17. Add 2 mL of the standard growth medium. Carefully remove the floating filter.

⚠ CRITICAL: If the filter does not spontaneously detach from the glass bottom hole into the medium, it is likely because too much PBS was removed before placing the filter. Forced removal of the filter often leads to loss of many cells. In this case, perform local UVC irradiation again using another dish.

18. Culture the cells for 10–60 min at 37°C.
19. Co-immunofluorescence staining with anti-GFP and anti-CPD antibodies.
    a. Wash the cells once with 1 mL of PBS.
    b. Incubate the cells for 10 min at 25°C with 1 mL of 2% paraformaldehyde (dilute 16% paraformaldehyde solution eight times with PBS just before use) and wash them three times with 1 mL of PBS.
    c. Incubate the cells for 10 min on ice with 1 mL of 0.5% Triton X-100 (dilute a 10% stock solution with PBS) and wash them three times with 1 mL of PBS.

    Note: Detergents such as Triton X-100 are used to permeabilize plasma membranes and thereby improve access of antibodies to cytoplasmic as well as nuclear antigens.

    d. For blocking nonspecific antibody binding, incubate the cells for 30 min at 37°C with 1 mL of 20% fetal bovine serum (FBS) (diluted with PBS).
    e. For staining GFP, dilute an anti-GFP rat antibody to a final concentration of 2 μg/mL with 5% FBS (diluted with PBS). Then, remove the blocking solution and incubate the cells for 16–20 h at 4°C with a sufficient amount of the primary antibody solution to cover the entire glass bottom surface (e.g., 100 μL for a 14 mm glass bottom hole).

    Note: Depending on the type of glass bottom dishes used, an appropriate volume of the antibody solution should be determined. To minimize evaporation and prevent the samples from drying out, dishes should be wrapped appropriately and/or incubated in a tight container.

    f. Wash the cells three times with 1 mL of PBS.
    g. Dilute an anti-rat IgG secondary antibody (Alexa Fluor 488-conjugated) to a final concentration of 2 μg/mL with 5% FBS. Then, incubate the cells for 30 min at 37°C with an appropriate volume of the secondary antibody solution (e.g., 100 μL for a 14 mm glass bottom hole).
    h. Wash the cells three times with 1 mL of PBS.
    i. Before acid-denaturation of genomic DNA required for the following CPD staining, it is crucial to fix the anti-GFP staining. Incubate the cells for 10 min at 25°C with 1 mL of 2% paraformaldehyde and then wash them three times with 1 mL of PBS.
    j. Incubate the cells for 20 min at 25°C with 1 mL of 2 M HCl (dilute 11.7 M HCl solution with PBS) and wash them three times with 1 mL of PBS.
    k. For blocking nonspecific antibody binding, add 1 mL of 20% FBS. Incubate the cells for 30 min at 37°C.
    l. For staining CPD, dilute an anti-CPD mouse antibody to a final concentration of 1 μg/mL with 5% FBS. Then, remove the blocking solution and incubate the cells for 30 min at 37°C with an appropriate volume of the primary antibody solution (e.g., 100 μL for a 14 mm glass bottom hole).
    m. Wash the cells three times with 1 mL of PBS.
    n. Dilute an anti-mouse IgG secondary antibody (Alexa Fluor 594-conjugated) to a final concentration of 2 μg/mL with 5% FBS. Then, incubate the cells for 30 min at 37°C with an appropriate volume of the secondary antibody solution (e.g., 100 μL for a 14 mm glass bottom hole).
    o. Wash the cells three times with 1 mL of PBS.
    p. For counterstaining of nuclear DNA, incubate the cells for 10 min at 25°C with 1 mL of PBS containing 1 μg/mL Hoechst 33342.
    q. Wash the cells three times with 1 mL of PBS.
    r. Mount the cells under a round coverslip (11 mm diameter) with 5 μL of Vectashield mounting medium (non-curing, without DAPI).

    Note: Anti-fade mounting media (such as Vectashield) prevent rapid photobleaching of fluorescent dyes/proteins during image acquisition, which is thus important for reproducibility.

Pause point: The mounting media also prevents drying out of the stained cells, and the mounted samples can be stored at 4°C in the dark for several days, or even longer if the edge of coverslips is sealed with plastic sealant or nail polish.

Alternatives: Other types of DAPI-free mounting media are also applicable. For instance, ibidi mounting media are designed such that covering with coverslips is unnecessary.

20. Microscopic observation.
    a. Turn on the confocal laser scanning fluorescence microscope, excitation lasers (405, 488, and 594 nm), and image acquisition software (e.g., FV31S-SW for Evident FV-3000).
    b. Select a 40× objective lens (UPlanSApo ×40, numerical aperture: 0.95) and focus on the sample.
    c. For acquiring fluorescence of Hoechst 33342, Alexa Fluor 488, and Alexa Fluor 594, set three channels with the parameters for excitation and emission as shown in the table below. Then, set the Airy Units to 1.00 AU in all channels.

	Excitation wavelength	Emission wavelength detected by photomultiplier tube (PMT)
Hoechst 33342	405 nm	430–470 nm
Alexa Fluor 488	488 nm	500–600 nm
Alexa Fluor 594	594 nm	610–710 nm

    d. Set image resolution to 1024 × 1024-pixels with 1× digital zoom (pixel size: 0.31 μm) and scan speed to 10 μsec/pixel.
    e. Set Lookup table (LUT) to Hi-Lo mode, which represents saturated fluorescence signals in red. Then, click "Live" to observe fluorescence signals.
    f. Adjust the laser powers to the appropriate values, such that all channels show substantial levels of fluorescence signals without saturation.

Note: To optimize the parameters for image acquisition, we usually tune up the laser powers only, while the sensitivity of PMT is fixed at 500 HV. Typically, starting points of the laser powers are 0.05% for Hoechst 33342 and Alexa Fluor 488, and 0.1% for Alexa Fluor 594. Once appropriate parameters are determined, it is crucial to apply the same imaging conditions for all samples that are compared directly.

    g. Acquire fluorescence images from a single focal plane and confirm the accumulation of EGFP-XPC at LUD sites, which are labeled by immunofluorescence signals of CPD (Figure 1D).

Note: We usually analyze over 50 cells in each time point from a single experiment.

KEY RESOURCES TABLE

REAGENT or RESOURCE	SOURCE	IDENTIFIER
Antibodies		
Rat monoclonal anti-GFP	Bio Academia	Cat#: 60-001
Mouse monoclonal anti-XPC (D-10)	Santa Cruz Biotechnology	Cat#: sc-74410; RRID: AB_1131407
Goat polyclonal anti-DDB2	R&D Systems	Cat#: AF3297; RRID: AB_2088829
Mouse monoclonal anti-α-tubulin (B-5-1-2)	Merck	Cat#: T5168; RRID: AB_477579
Mouse monoclonal anti-acetyl histone H3 (Lys27) (MABI0309)	Fujifilm Wako Pure Chemical	Cat#: 308-34843
Rabbit polyclonal anti-histone H3 (pan-H3)	Abcam	Cat#: ab1791; RRID: AB_302613

(*Continued on next page*)

Continued

REAGENT or RESOURCE	SOURCE	IDENTIFIER
Mouse monoclonal anti-CPD (TDM-2)	Cosmo Bio	Cat#: NM-DND-001; RRID: AB_1962813
Mouse monoclonal anti-6-4PP (64M-2)	Cosmo Bio	Cat#: NM-DND-002; RRID: AB_1962842
Goat anti-rat IgG (H + L) secondary antibody, Alexa Fluor 488-conjugated	Thermo Fisher Scientific	Cat#: A-11006; RRID: AB_2534074
Goat anti-mouse IgG (H + L) secondary antibody, Alexa Fluor 405-conjugated	Thermo Fisher Scientific	Cat#: A-31553; RRID: AB_221604
Goat anti-mouse IgG (H + L) secondary antibody (Fab'), Alexa Fluor 594-conjugated	Thermo Fisher Scientific	Cat#: A-11020; RRID: AB_2534087
Goat anti-rabbit IgG (H + L) secondary antibody, Alexa Fluor 594-conjugated	Thermo Fisher Scientific	Cat#: A-11037; RRID: AB_2534095
Bacterial and virus strains		
Recombinant retrovirus expressing FLAG-EGFP-XPC^{WT}	Kusakabe et al.[1]	N/A
Chemicals, peptides, and recombinant proteins		
FuGENE HD transfection reagent	Promega	Cat#: E2311
Experimental models: Cell lines		
U2OS cell lines (WT, DDB2 KO, XPC KO)	Sakai et al.[13]	N/A
U2OS^{WT} cells stably expressing FLAG-EGFP-XPC	Kusakabe et al.[1]	N/A
U2OS$^{DDB2\ KO}$ cells stably expressing FLAG-EGFP-XPC	Kusakabe et al.[1]	N/A
293-GPG	Ory et al.[11]	N/A
Recombinant DNA		
pMMP-puro/FLAG-EGFP-XPC	Kusakabe et al.[1]	N/A
Software and algorithms		
FV31S-SW	Evident	https://www.olympus-lifescience.com/en/support/downloads/fv3000_vw_license/
Fiji/ImageJ	Schindelin et al.[14]	https://imagej.net/software/fiji/
MATLAB	MathWorks	https://www.mathworks.com/products/matlab.html
GraphPad Prism 9	GraphPad Software	https://www.graphpad.com/scientific-software/prism/
Other		
Millex-HV PVDF filter, 0.45 μm pore size	Merck	Cat#: SLHVJ13SL
Cryotube (2 mL)	TPP	Cat#: 89020
Glass bottom dish (35 mm, poly-D-lysine coated)	MatTek	Cat#: P35GC-1.5-14-C/H
Polycarbonate isopore membrane filter, 5 μm pore size	Merck	Cat#: TMTP01300
Vectashield mounting medium	Vector Laboratories	Cat#: H-1000
Micro cover glass (round shape, 11 mm diameter, 0.13–0.17 mm thickness)	Matsunami Glass Industry	N/A This is a made-to-order product from Matsunami Glass Industry.
96-Well glass bottom plate	Matsunami Glass Industry	Cat#: GP96000
Stripwell microplate, 1 × 8 well	Corning	Cat#: 9102
Dulbecco's modified Eagle medium (DMEM) powder (autoclavable, without L-glutamine and $NaHCO_3$)	Nissui Pharmaceutical	Cat#: 05919
Fetal bovine serum (FBS)	Corning	Cat#: 35-079-CV
Dulbecco's phosphate buffered saline, PBS (-)	Nissui Pharmaceutical	Cat#: 05913
0.5% (w/v) Trypsin-5.3 mM EDTA·4Na solution, without phenol red (× 10)	Fujifilm Wako Pure Chemical	Cat#: 208-17251
Sodium bicarbonate ($NaHCO_3$)	Fujifilm Wako Pure Chemical	Cat#: 191-01305
L(+)-Glutamine	Fujifilm Wako Pure Chemical	Cat#: 078-00525
Bottle top vacuum filter, 0.22 μm pore size	Corning	Cat#: 430624
Benzylpenicillin potassium	Fujifilm Wako Pure Chemical	Cat#: 021-07732
Streptomycin sulfate	Fujifilm Wako Pure Chemical	Cat#: 194-08512
Puromycin dihydrochloride (1 mg/mL solution)	Merck	Cat#: P9620-10ML

(*Continued on next page*)

Continued

REAGENT or RESOURCE	SOURCE	IDENTIFIER
Geneticin (50 mg/mL solution)	Thermo Fisher Scientific	Cat#: 10131035
Tetracycline hydrochloride	Nacalai Tesque	Cat#: 330-31
Paraformaldehyde, 16% (w/v) aqueous solution, methanol free	Fujifilm Wako Pure Chemical	Cat#: 043368
Polyoxyethylene (10) octylphenyl ether (Triton X-100)	Fujifilm Wako Pure Chemical	Cat#: 160-24751
Germicidal lamp with a peak wavelength of 254 nm	Toshiba	Cat#: GL-15
Hoechst 33342 (1 mg/mL in H_2O)	Dojindo Laboratories	Cat#: H342
Propidium iodide (1 mg/mL in H_2O)	Merck	Cat#: P4864-10ML
FV-3000 confocal laser microscope equipped with high sensitivity spectral PMT detectors (FV31-HSD), dichroic mirrors (DM405/488/594 and DM405/488/561), and a scan unit (FV31-SU)	Evident	https://www.olympus-lifescience.com/ja/laser-scanning/fv3000/
Objective lens UPlanSApo ×20 (numerical aperture: 0.75)	Evident	Product name: UPLSAPO20X
Objective lens UPlanSApo ×40 (numerical aperture: 0.95)	Evident	Product name: UPLSAPO40X
114 × 75 mm travel stepper motor XY stage	Prior	https://www.prior.com/product/h117
OBIS LX lasers (405, 488, 561, and 594 nm)	Coherent	https://coherentinc.my.site.com/Coherent/lasers/lasers-laser-systems/obis-lx-ls?cclcl=en_US

MATERIALS AND EQUIPMENT

Materials

- Dulbecco's Modified Eagle's Medium (DMEM): 4.75 g of DMEM powder (L-glutamine- and sodium bicarbonate-free) is dissolved in 400 mL of ultrapure water, and the volume is then adjusted to 500 mL with ultrapure water. The solution is sterilized by autoclaving at 121°C for 20 min. Before use, an appropriate amount (approximately 6 mL) of 10% sodium bicarbonate and 10 mL of 200 mM L-glutamine solutions (both sterilized with 0.22 μm pore filters) are added.
- 100× Antibiotics stock solution: 7.0 g of streptomycin sulfate and 3.3 g of benzylpenicillin potassium are dissolved in 400 mL of ultrapure water. The volume is adjusted to 500 mL with ultrapure water. After sterilization with a 0.22 μm pore filter, 40 mL aliquots are stored at -20°C.

Standard growth medium

Reagent	Final concentration	Amount
DMEM	N/A	Approx. 516 mL
100× Antibiotics stock solution	1 ×	5 mL
FBS	10% v/v	57 mL
Total	**N/A**	**Approx. 578 mL**

Store at 4°C.

Note: The addition of antibiotics to the culture medium is optional. We routinely use antibiotics, considering that some experiments, such as transfection and UV irradiation, may not be performed under completely sterile conditions.

293-GPG maintaining medium

Reagent	Final concentration	Amount
Standard growth medium	N/A	100 mL
10 mg/mL Tetracycline	1 μg/mL	10 μL

(*Continued on next page*)

Continued		
Reagent	Final concentration	Amount
10 mg/mL Puromycin	2 μg/mL	20 μL
50 mg/mL Geneticin	0.3 mg/mL	600 μL
Total	N/A	Approx. 100 mL
Store at 4°C.		

Pre-extraction buffer		
Reagent	Final concentration	Amount
250 mM PIPES-NaOH (pH 6.8)	10 mM	4 mL
5 M NaCl	100 mM	2 mL
Sucrose	300 mM	10.3 g
1 M $MgCl_2$	3 mM	300 μL
500 mM EGTA-NaOH (pH 8.0)	1 mM	200 μL
10% (v/v) Triton X-100	0.5% v/v	5 mL
Ultrapure water	N/A	The final volume is adjusted to 100 mL with ultrapure water
Total	N/A	100 mL
Store at 4°C.		

Equipment

For microscopic observation described in this paper, we use the confocal laser scanning microscope FV-3000 (Evident). Our system is equipped with high sensitivity spectral PMT detectors (FV31-HSD; Evident), dichroic mirrors (DM405/488/594 and DM405/488/561; Evident), a scan unit (FV31-SU; Evident), and objective lenses UPlanSApo ×20 (numerical aperture: 0.75) and UplanSApo ×40 (numerical aperture: 0.95). For acquisition of fluorescence signals, 405, 488, 561, and 594 nm OBIS LX lasers (Coherent) are used and setting of the parameters for excitation and emission is described in each experimental procedure. In addition, to evaluate the repair kinetics of 6-4PPs, an electrically operated XY stage (e.g., 114 × 75 mm travel stepper motor XY stage; Prior) is useful for choosing the correct position in a 96-well glass bottom plate and also for possible automated analyses in future. However, conventional wide-field fluorescence microscopes are also applicable, as far as sufficient levels of sensitivity and quantitativeness of fluorescence detection are achieved.

Following the protocols described in this paper, we usually obtain a fluorescence image from a single focal plane at each location. The estimated XY- and Z-axis resolution of a focal plane, which is calculated by the Nikon Resolution Calculator (https://www.microscope.healthcare.nikon.com/microtools/resolution-calculator/), is shown in the table below. In this calculation, other parameters such as Modality (Point-Scanning), Active Pixels (1024 × 1024), and Airy Units (1.00 AU) are fixed.

			20× objective lens		40× objective lens	
Excitation wavelength	Emission wavelength	Example of fluorescence dye	XY-axis	Z-axis	XY-axis	Z-axis
405 nm	450 nm	Hoechst 33342, etc.	320 nm	1149 nm	252 nm	716 nm
488 nm	550 nm	Alexa Fluor 488, etc.	385 nm	1385 nm	304 nm	863 nm
561 nm	660 nm	PI, etc.	443 nm	1592 nm	349 nm	992 nm
594 nm	660 nm	Alexa Fluor 594, etc.	469 nm	1686 nm	370 nm	1051 nm

STEP-BY-STEP METHOD DETAILS

Assessing the localization of factors of interest at LUD sites

Here, we describe a method to quantitatively evaluate the localization of factors of interest upon local UVC exposure. This method consists of the following two procedures: 1) immunofluorescence

microscopy combined with local UV irradiation (described above), and 2) quantitative image analysis.

Cell culture and local UVC irradiation

Timing: 2 days

The following steps enable induction of UV-induced photolesions to local subnuclear area.

1. Trypsinize U2OS cells stably expressing EGFP-XPC and measure the cell density with a hemocytometer.
2. Plate 3.0×10^5 cells per 35 mm glass bottom dish and culture the cells for 16–20 h.

   Optional: If any protein of interest needs to be expressed transiently by plasmid transfection, 1.0×10^5 cells are usually seeded in a 35 mm glass bottom dish and cultured for 16–20 h. After transfection with 2 μg of the expression construct, cells are cultured for additional 2 days and subjected to the following UVC irradiation. For the details and an example of such experiments, refer to our previous paper.[1]

3. Local UVC irradiation through polycarbonate isopore membrane filters (Figure 1C).
   a. Irradiate the cells with UVC through the filter as described above (refer to the section 'confirmation of the functionality of EGFP-XPC by immunofluorescence staining').
   b. Add 2 mL of the standard growth medium. Carefully remove the floating filter.
   c. Culture the cells at 37°C for the desired time period.

Immunofluorescence staining and microscopic observation

Timing: 2 days

The following steps are aimed at visualizing localization of the factors of interest at LUD sites.

4. Wash the cells twice with 1 mL of PBS.
5. Fixation.

   Optional: In some cases, it is worth considering that cells are first incubated on ice for 20 min with 1 mL of the pre-extraction buffer and then immediately subjected to paraformaldehyde fixation. This washes out proteins in the nucleoplasm or loosely bound to chromatin, so that relatively weak localization at LUD sites may become more evident.

   a. Incubate the cells for 10 min at 25°C with 1 mL of 2% paraformaldehyde.
   b. Wash the cells twice with 1 mL of PBS.
6. Permeabilization.
   a. Incubate the cells for 10 min on ice with 1 mL of 0.5% Triton X-100.
   b. Wash the cells twice with 1 mL of PBS.
7. Incubate the cells for 30 min at 37°C with 1 mL of 20% FBS to block nonspecific antibody binding.
8. Primary antibody reaction.
   a. Wash the cells twice with 1 mL of PBS.
   b. Dilute the primary antibody recognizing the target protein of interest with 5% FBS to an appropriate concentration.

   Note: In our previous study (Kusakabe et al., 2022), for instance, we used anti-acetyl histone H3 (Lys27) (Clone#: MABI0309) at a final concentration of 1 μg/mL.[1] We usually start with this

antibody concentration, while it may need to be adjusted experimentally depending on the target protein and antibody used.

c. Incubate the cells for 16–20 h at 4°C with an appropriate volume of primary antibody solution (e.g., 100 μL for a 14 mm glass bottom hole).
d. Wash the cells five times with 1 mL of PBS.

9. Secondary antibody reaction.
   a. Incubate the cells for 30 min at 37°C with an appropriate volume of 5% FBS containing 4 μg/mL Alexa Fluor 594-labeled secondary antibody (e.g., 100 μL for a 14 mm glass bottom hole).
   b. Wash the cells five times with 1 mL of PBS.
10. Counterstaining.
   a. Incubate the cells for 10 min at 25°C with 1 mL of PBS containing 1 μg/mL Hoechst 33342.
   b. Wash the cells five times with 1 mL of PBS.
11. Mount the cells under a round coverslip (11 mm diameter) with 5 μL of the Vectashield mounting medium.

Note: After preparing the immunofluorescence samples, we usually proceed to the following microscopic observation immediately. If it is necessary to store the samples, refer to the Note in the section: 'confirmation of the functionality of EGFP-XPC by immunofluorescence staining step 19-r'.

12. Turn on the confocal laser scanning microscope, excitation lasers (405, 488, and 594 nm), and image acquisition software.

Note: For the image acquisition procedure described below, we use the FV-3000 confocal laser scanning microscope and accompanying FV31S-SW software (Evident). The detail of the microscopic system is described in 'Materials and Equipment'.

13. Select a 40× objective lens (UplanSApo ×40, numerical aperture: 0.95) and focus on the sample.
14. For acquisition of fluorescence images of Hoechst 33342, EGFP, and Alexa Fluor 594, set three channels with the parameters for excitation and emission as shown in the table below. Then, set the Airy Units to 1.00 AU in all channels.

	Excitation wavelength	Emission wavelength detected by PMT
Hoechst 33342	405 nm	430–470 nm
EGFP	488 nm	500–600 nm
Alexa Fluor 594	594 nm	610–710 nm

15. Set image resolution to 1024 × 1024-pixels with 1× digital zoom (pixel size: 0.31 μm) and scan speed to 10 μsec/pixel.
16. Set LUT to Hi-Lo mode and click "Live" to display the fluorescence signals.
17. Adjust the laser powers to the appropriate values, such that all channels show substantial levels of fluorescence signals without saturation.

Note: We usually tune up the laser powers only, while the sensitivity of PMT is fixed at 500 HV. Typically, starting points of the laser powers are 0.05% for Hoechst 33342 and EGFP, and 0.01% for Alexa Fluor 594.

18. Acquire fluorescence images from a single focal plane (Figures 2A and 2B).

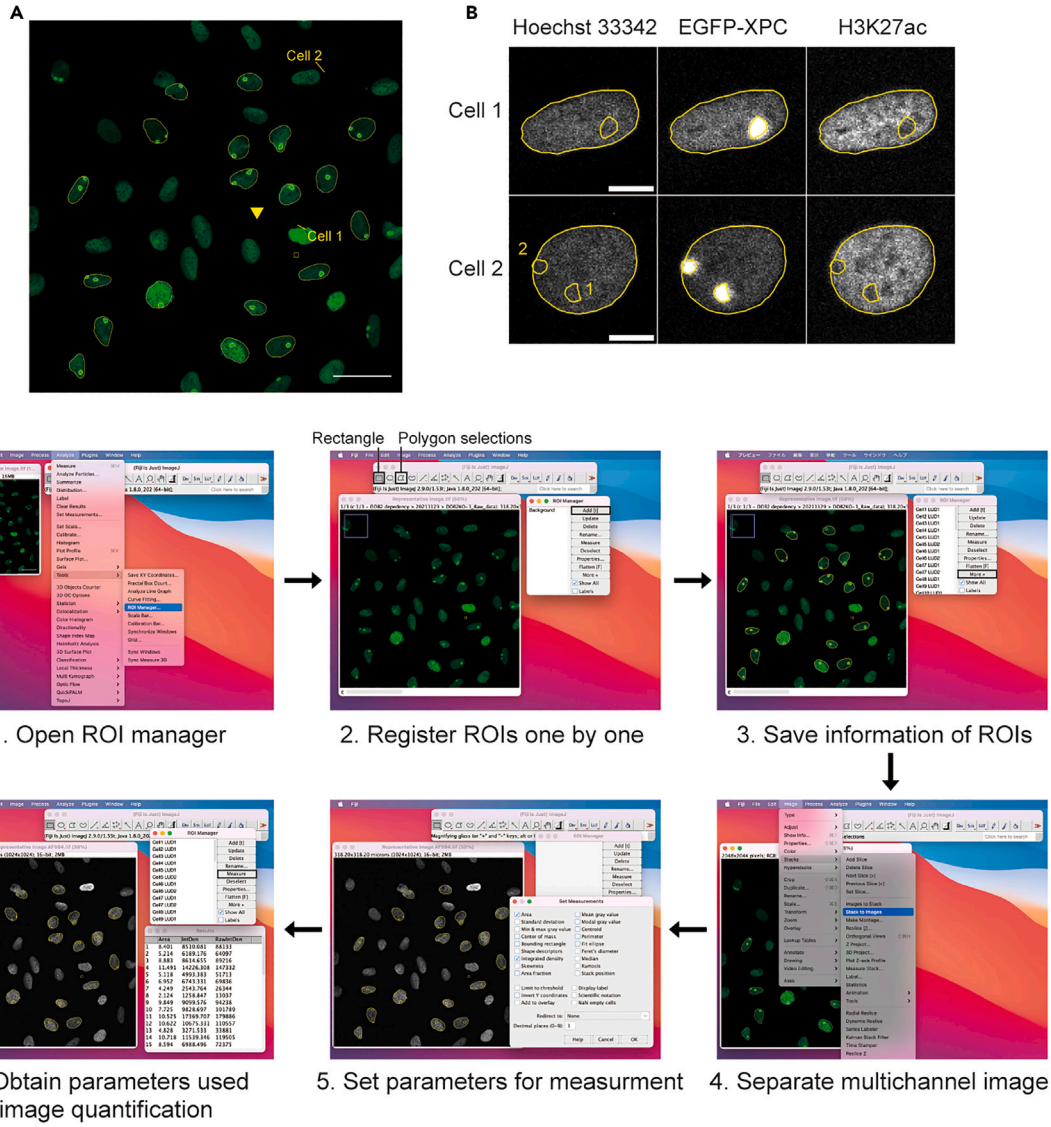

D

		Area (Pixels)	Total FI	Mean FI per pixel	Background subtracted	Relative FI at LUD
Background		144	30678	213		
Cell1	LUD	131	145806	1113	900	0.801
	Nucleus	2738	3659910	1337	1124	
Cell2	LUD1	104	108352			
	LUD2	82	79779			
	Total LUDs	186	188131	1011	798	0.742
	Nucleus	3636	4683058	1288	1075	

Figure 2. Image analyses for assessing the localization of factors of interest at LUD sites

(A) U2OS$^{DDB2\ KO}$ cells stably expressing EGFP-XPC were irradiated with UVC (400 J/m^2) through the isopore membrane filter. After incubation for 30 min, cells were fixed and subjected to immunofluorescence staining with an anti-H3K27ac antibody. A representative image of EGFP fluorescence is shown. Based on the EGFP signals, UV-irradiated areas and the corresponding nuclei were demarcated and set as ROIs. The yellow arrowhead indicates a ROI used as background. Scale bar: 50 μm.

(B) Enlarged fluorescence images of Cells 1 and 2 shown in (A). Scale bars: 10 μm.

Figure 2. *Continued*

(C) Schematic representation of the image quantification with Fiji/ImageJ. As a model analysis, the immunofluorescence image shown in (A) was used. After the image was selected, ROI manager was opened (1). ROIs were determined and registered to ROI manager by clicking "add [t]" (bold circle) (2). After registering all ROIs, the information of ROIs was saved by clicking "More" (bold circle) and "Save…" (3). For choosing the fluorescence signal of factors of interest, the multichannel image was separated, and the signal of Alexa Fluor 594 was picked up (4). Then, the parameters used for image quantification were selected in "Set measurements" and obtained by clicking "Measure" (bold circle) (5–6).

(D) Quantification of the relative fluorescence intensity (FI) of H3K27ac in Cells 1 and 2. The area and total FI were measured for each ROI, and the mean FI per pixel was calculated by dividing the total FI by the area. If there were multiple LUD sites like in Cell 2, the sums of the area and total FI were used to calculate the mean FI at LUD sites. The relative FI at LUD sites was calculated by the formula described in 27 of the section titled 'step-by-step method details'.

Image analysis with ImageJ

Timing: 1 day

The following image analyses accomplish a quantitative assessment of localization of the factors upon local UVC irradiation.

19. Open the acquired multichannel image with Fiji/ImageJ.[14]

Note: We confirmed that the image quantification procedure described below works in Fiji which builds on ImageJ2 version 2.9.0/1.53t.

20. Determine three regions of interest (ROIs) as follows: 1) the UVC-irradiated area demarcated with fluorescence of EGFP-XPC (D), 2) the entire cell nucleus (N), and 3) the area outside of any cell as a background (BKG) (Figures 2A–2C).
    a. For opening ROI manager, click "analyze," "tools," and "ROI manager…" (Figure 2C).
    b. In ImageJ toolbar, choose "Rectangle" to determine a ROI for BKG, or "Polygon selections" to determine ROIs for D and N (Figure 2C).
    c. After creating a ROI, click "Add [t]" and register it in the ROI manager one by one (Figure 2C).
    d. After finishing registration of all ROIs, click "More" and "Save…" and then save the ROI data. Keep opening the data of ROIs until extracting fluorescence of Alexa Fluor 594 (Figure 2C).

Alternatives: Although we manually determine each ROI, an alternative method has been recently developed, which is based on ImageJ macro and automatically determines regions of LUD sites.[15]

21. Separate the multichannel image into individual fluorescence images by clicking "Image," "Stacks," and "Stack to Images" (Figure 2C).
22. Select the Alexa Fluor 594 fluorescence image.
23. To register the parameters for measurement, click "Analyze" and "Set Measurements…" and select "Area" and "Integrated density," which represents total fluorescence intensity (Figure 2C).
24. For acquiring the fluorescence intensity in each ROI, click "Measure" in ROI manager toolbar and save the results as a csv file (Figure 2C).
25. Open the results file, and then copy and paste the data (Label, Area, and Integrated density) into a new Excel file.
26. Determine the mean fluorescence intensities per pixel by dividing the integrated density by the area in Excel software. Then, define the mean fluorescence intensity per pixel corresponding to D, N, and BKG as F_D, F_N, and F_{BKG}, respectively (Figure 2D).
27. Calculate the relative fluorescence intensities at the LUD site (F_R) using the following formula:

$$F_R = \frac{(F_D - F_{BKG})}{(F_N - F_{BKG})}$$

Note: We usually analyze over 50 cells in each condition from a single experiment.

Note: In this protocol, we define LUD sites by the areas with accumulating EGFP fluorescence. As with the description in the steps of Before you begin 12–20, monoclonal antibodies against UV-induced photolesions generated in mice have been widely used to demarcate UVC-irradiated regions by immunofluorescence staining.[16] However, because many reliable monoclonal antibodies against histone modifications were also generated in mice,[17] the simultaneous use of these antibodies for immunofluorescence staining is difficult. To circumvent such a problem, we choose EGFP-XPC as a marker of LUD sites in this protocol.

Assessing the repair kinetics of UV-induced 6-4PPs in cultured cells

Here, we describe a method that is applicable for assessing the kinetics of removal of UV-induced 6-4PPs in cultured cells. This method mainly consists of the following three procedures: 1) global UVC irradiation of cells cultured in a 96-well plate, 2) immunofluorescence microscopy, and 3) quantitative image analysis.

Cell culture and global UVC irradiation

Timing: 2 days

The following steps enable global UVC irradiation to cultured cells in a 96-well glass bottom plate.

28. Trypsinize U2OS cells and measure the cell density with a hemocytometer.
29. Plate 3.0×10^4 cells per well of a sterile 96-well glass bottom plate (non-coated, glass thickness: 0.16–0.19 mm, GP96000, Matsunami Glass Industry). Then, culture the cells for 16–20 h.

Note: Appropriate treatment of the glass bottom plate may be necessary depending on cell lines used.

30. UVC irradiation to assess repair kinetics.

Note: Cells seeded on the same plate may need to be treated with UVC at different doses and/or timings. To this end, we use a 96-strip-well microplate as a cover to protect cells in unintended wells from UVC. With this method, therefore, experiments should be designed such that cells in the same column of a plate are treated simultaneously with the same dose of UVC. It is also important to confirm that the two plates have the same well positions.

    a. Using a multichannel micropipette, carefully remove the growth medium from a column of wells that are subjected to UVC irradiation (Figure 3A).
    b. Corresponding to the intended column position, remove an 8-well strip from the strip-well plate. Overlay the strip-well plate on the glass bottom plate containing cells (Figure 3B).
    c. Irradiate the cells with UVC at a dose of 10 J/m^2 (Figure 3C).
    d. Add 150 μL of the fresh standard growth medium to each well and incubate the plate at 37°C (Figure 3C).
    e. After 60 and 90 min, treat the cells in different columns of the 96-well glass bottom plate according to the procedure described in a–d (Figure 3C).
    f. Further incubate the plate at 37°C so that the recovery times after UV irradiation for individual columns are set to 30, 60, and 120 min, respectively.

Note: UV irradiation at the time points of 0, 60, and 90 min corresponds to the recovery time for 120, 60, and 30 min, respectively. By shifting the timing of UVC irradiation in this way, all wells in the plate can be subjected to the following procedures in parallel.

    g. Transfer the plate on ice (Figure 3C).

31. UVC irradiation to prepare a standard curve for lesion quantification (Figure 3C).

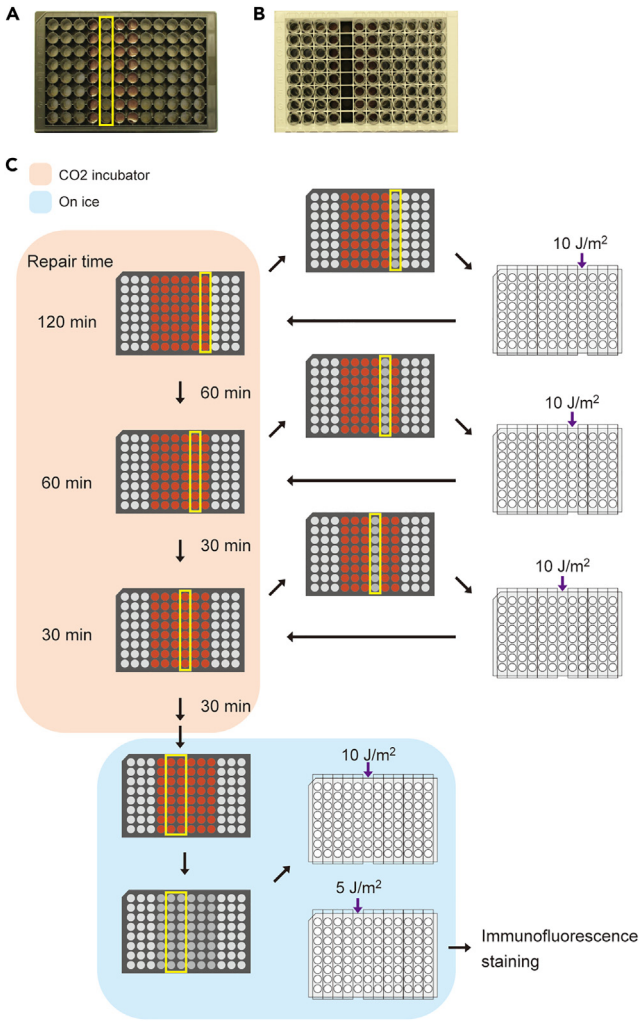

Figure 3. Schematic procedure for UVC irradiation using a 96-well glass bottom plate

(A) Before global UVC irradiation, the medium was removed from a column of wells subjected to UVC irradiation (indicated by the yellow square).

(B) An 8-strip well corresponding to the column for UVC irradiation was removed from the strip-well plate. During UVC irradiation, the 96-well glass bottom plate was overlaid with the strip-well plate to protect unintended wells from UVC.

(C) To align the finishing time of the recovery culture, the timing of UVC irradiation was shifted for different columns, as shown in this figure. For each column of wells, the medium was removed, and UVC was irradiated through the cover of the strip-well plate. After fresh growth medium was added, the cells were incubated at 37°C for the desired time period. At the end of the recovery culture, the 96-well glass bottom plate was transferred on ice. To prepare the standard curve, UVC irradiation (5 and 10 J/m^2) was performed with the cells kept on ice, and then the whole plate underwent immunofluorescence staining. Columns subjected to UV irradiation are labeled by yellow squares.

a. Remove the medium from three columns of wells containing unirradiated cells.
b. Keep the plate on ice and irradiate the cells in individual columns with UVC at doses of 5 and 10 J/m^2.
c. After finishing the UVC irradiation, immediately proceed to the following immunofluorescence staining.

Immunofluorescence staining with lesion-specific antibodies and microscopic observation

Timing: 2 days

The procedures described below achieve acquiring fluorescence images of 6-4PPs and DNA for quantitative image analysis.

32. Fixation.
    a. Incubate the cells for 10 min at 25°C with 2% paraformaldehyde (150 μL per well).
    b. Wash the cells three times with PBS (150 μL per well).
33. Permeabilization.
    a. Incubate the cells for 10 min at 25°C with PBS containing 0.5% Triton X-100 (150 μL per well).
    b. Wash the cells three times with PBS (150 μL per well).
34. Denaturation of genomic DNA.
    a. Incubate the cells for 20 min at 25°C in 2 M HCl (150 μL per well).
    b. Wash the cells three times with PBS (150 μL per well).
35. For blocking nonspecific antibody binding, add 20% FBS (150 μL per well) and incubate the cells for 30 min at 25°C.
36. Primary antibody reaction.
    a. Dilute an anti-6-4PP mouse antibody to a final concentration of 0.5 μg/mL with 5% FBS and incubate the cells for 16–20 h at 4°C with the primary antibody solution (50 μL per well).

    Note: An appropriate volume of the antibody solution should be determined. To minimize evaporation and prevent the samples from drying out, a 96-well glass bottom plate should be wrapped appropriately and/or incubated in a tight container.

    b. Wash the cells three times with PBS (150 μL per well).
37. Secondary antibody reaction.
    a. Dilute an Alexa Fluor 405-labeled anti-mouse IgG secondary antibody to a final concentration of 2 μg/mL with 5% FBS and incubate the cells for 60 min at 25°C with the secondary antibody solution (50 μL per well).
    b. Wash the cells three times with PBS (150 μL per well).
38. Counterstaining.
    a. Stain nuclear DNA for 20 min at 25°C with PBS containing 1 μg/mL propidium iodide (PI) (50 μL per well).
    b. Wash the cells three times with PBS (150 μL per well).
    c. Fill each well with 100 μL of PBS to prevent the cells from drying out.
39. Turn on the confocal laser scanning microscope, excitation lasers (405 and 561 nm), and image acquisition software.
40. Select a 20× objective lens (UplanSApo ×20, numerical aperture: 0.75) and focus on the sample.
41. For acquisition of fluorescence images of Alexa Fluor 405 and PI, set two channels with the parameters for excitation and emission as follows.

	Excitation wavelength	Emission wavelength detected by PMT detector
Alexa Fluor 405	405 nm	430–470 nm
PI	561 nm	610–710 nm

42. Set the image resolution to 1024 × 1024-pixels with 1× digital zoom (pixel size: 0.62 μm) and the scan speed to 20 μsec/pixel.
43. Set the Airy Units to 7.67 AU for Alexa Fluor 405 and to 5.25 AU for PI.

Note: The default setting of the Airy Unit is 1.00 AU. By changing the parameters like this, the thickness of a focal plane of Alexa Fluor 405 is increased from 1149 nm to 1440 nm, and that of

PI is increased from 1592 nm to 1995 nm. This increases a fraction of fluorescence captured, thereby improving accuracy of the following quantitative analysis.

44. Set LUT to Hi-Lo mode and click "Live" to display the fluorescence signals.
45. By checking the fluorescence images of cells which were irradiated with UVC at 10 J/m^2 and fixed immediately, adjust the laser powers to the appropriate values, such that both channels show substantial levels of fluorescence signals without saturation.

Note: We usually tune up the laser powers only, while the sensitivity of PMT is fixed at 500 HV. Typically, starting points of the laser powers are 3.0% for Alexa Fluor 405 and 0.01% for PI.

46. Set a ROI for image acquisition such that it mainly covers the central part but excludes the edge in each field of view (with a 20× objective lens, we usually set a ROI of 695 × 695 pixels near the center).
47. Acquire fluorescence images from a single focal plane. We acquire at least three fluorescence images of different positions from each well.

Note: We usually select a position, in which over 50 cells are observed.

Image analysis with MATLAB

Timing: 1 day

The following image analysis enables semi-quantification of the amount of 6-4PPs in each cell and assessment of kinetics of removal of 6-4PPs.

Alternatives: Herewith we describe a method with the MATLAB code, which was used in our recent work.[1] Basically the same analysis is possible with a free/open source software such as ImageJ, CellProfiler and so on.[14,18] A Fiji/ImageJ-based program as well as the results using it are provided as Supplemental information (Methods S1, Figures S1 and S2).

48. Split the multichannel image into individual fluorescence images and save the images as TIFF files.
49. Open and show the acquired fluorescence images with MATLAB by using the following code (Figures 4A and 4B).

Note: In this code, "name of the fluorescence image of Alexa Fluor 405" and "name of the fluorescence image of PI" should be replaced by the appropriate file names, respectively.

```
alexa = imread(''name of the fluorescence image of Alexa Fluor 405'');

DNA = imread(''name of the fluorescence image of PI'');

alexa_adj = imadjust(alexa);

DNA_adj = imadjust(DNA);

figure(1), imshowpair(alexa_adj, DNA_adj, 'montage');
```

50. Binarize the fluorescence image of PI to determine ROIs corresponding to individual cell nuclei (Figure 4B).

```
DNA_BW = imbinarize(DNA, 'adaptive', 'Sensitivity', 0.8)
figure(2), imshowpair(DNA, DNA_BW, 'montage')
```

51. Remove the signal noise and fill the gap in the nucleus (Figure 4B).

```
figure(3), subplot(1,3,1), imshow(DNA_BW);title('Pre-treatment');
DNA_BW2 = bwareaopen(DNA_BW, 10);
DNA_BW2 = imopen(DNA_BW2, strel('disk',2));
subplot(1,3,2), imshow(DNA_BW2);title('Post-removing noise');
DNA_BW2 = imfill(DNA_BW2, 'hole');
DNA_BW2 = medfilt2(DNA_BW2, [3 3]);
subplot(1, 3, 3), imshow(DNA_BW2);title('Post-gap filling');
```

52. Label each ROI (Figure 4B).

```
label = bwlabel(DNA_BW2);
figure(4), imshow(label2rgb(label, 'jet', 'k', 'shuffle'));
```

53. Distinguish attached cells by watershed conversion (Figure 4B).

```
DNA_Dist = -bwdist(~DNA_BW2);
DNA_Nmin = imhmin(DNA_Dist, 1.3);
DNA_Seg = watershed(DNA_Nmin);
DNA_Seg(~DNA_BW2) = 0;
figure(5), imshowpair(label2rgb(label,'jet','k', 'shuffle'), ...
label2rgb(DNA_Seg,'jet','k', 'shuffle'), 'montage');
```

54. Remove nuclei that are small or located at the edge of the image.

```
BWSeg = DNA_Seg > 0;
BWSeg = bwareafilt(BWSeg, [100,3000]);
BWSeg = imclearborder(BWSeg);
regionNum = max(max(bwlabel(BWSeg)));
figure(6), imshow(DNA_adj); hold on;
im = visboundaries(BWSeg);
```

55. Obtain information of morphology of individual ROIs.

```
stats = regionprops(BWSeg, 'Area', ...
'BoundingBox', ...
'Centroid', ...
'Perimeter', ...
'PixelIdxList');
areas = [stats.Area]';
centroids = cat(1, stats.Centroid);
perimeters = [stats.Perimeter]';
circularity = 4*pi*areas ./ perimeters.^2;
```

56. Remove the attached cells by evaluating circularity and area of the ROIs (Figure 4B).

```
inds_false = areas > 900 & circularity < 0.7;
falseBW = zeros(size(DNA));
TrueBW = zeros(size(DNA));
for i = 1:length(stats)
if inds_false(i)
falseBW(stats(i).PixelIdxList) = 1;
else
TrueBW(stats(i).PixelIdxList) = 1;
end
end
figure(7), imshow(DNA_adj); hold on;
visboundaries(falseBW, 'Color', 'red');
visboundaries(TrueBW, 'Color', 'green');
```

57. For each ROI, determine the relative fluorescence intensity of 6-4PPs (designated as X), which is calculated by dividing the mean fluorescence intensity per pixel of 6-4PPs by that of PI.

Note: To confirm the correlation between the fluorescence intensity of Alexa Fluor 405 and that of PI, we usually prepare scatter plots using the following MATLAB code (Figure 4C).

```
statsTrue = stats(~inds_false);
for i = 1:nnz(~inds_false)
mean_intensity_alexa(i) = mean(alexa(statsTrue(i).PixelIdxList));
mean_intensity_DNA(i) = mean(DNA(statsTrue(i).PixelIdxList));
end
X = mean_intensity_alexa./mean_intensity_DNA;
figure(8); grid on; hold on;
```

```
scatter(mean_intensity_DNA, mean_intensity_alexa, 'r.');
xlabel('Mean intensity of PI');
ylabel('Mean intensity of Alexa');
```

58. Open the work space, and copy and paste the relative intensity of 6-4PPs in each cell into an Excel file.
59. Calculate the median of the relative intensity of 6-4PPs in each image. By using the medians, prepare a standard curve and determine the amount of 6-4PPs after recovery culture for the indicated time periods.

Note: The method for preparing a standard curve and calculating the amount of 6-4PPs is described in the section 'quantification and statistical analysis'.

EXPECTED OUTCOMES

Assessing the localization of factors of interest at LUD sites

After cells stably expressing EGFP-XPC were irradiated with UVC through the isopore membrane filter and subjected to immunofluorescence staining, we confirmed the accumulation of EGFP-XPC at LUD sites at 10, 30, and 60 min post-irradiation (Figure 5A). Although the percentage of cells with EGFP-XPC accumulating at LUD sites is unaffected by the absence and presence of UV-DDB at 10 min after irradiation, it is modestly decreased in DDB2-knockout (KO) cells at 30 and 60 min after irradiation (Figure 5B; left graph). This is probably because the accumulation of XPC to LUD sites depends mostly on remaining 6-4PPs, while persisting CPDs refrain from recognition by XPC especially in the absence of DDB2. However, it should be noted that the sites with XPC accumulation unexceptionally coincided with intense CPD signals at all time points regardless of the presence or absence of UV-DDB (Figure 5B; right graph). This indicates that accumulation of EGFP-XPC can be used to mark LUD sites instead of CPD staining, although care should be taken if relatively long post-UV incubation is required with UV-DDB-deficient cells.

By using a combination of local UV irradiation and immunofluorescence staining, a decrease in the H3K27ac level at LUD sites was observed in U2OS cells, while the signal of H3 was not altered, at 30 min after irradiation, indicating that histone deacetylation is induced at LUD sites (Figures 2B and 2D).[1] Consistently, the recruitment of HDAC2 and its catalytic activator metastasis-associated (MTA) proteins to LUD sites was observed.[1] Taken together, these findings demonstrate that this method is applicable for assessing the relocalization of the factors upon UVC irradiation.

Assessing the repair kinetics of UV-induced 6-4PPs in cultured cells

The protocol for indirect immunofluorescence staining of UV-induced photolesions has already been established.[19] Although this method has been applied to quantify DNA photolesions in cell populations, its usefulness for individual cell analysis has not been evaluated in detail. Figure 6A shows representative images of cells irradiated with UVC and subjected to immunofluorescence staining. For this type of assay, it should always be kept in mind that the level of lesions present in a certain amount of DNA is reduced twice by DNA replication even in the absence of DNA repair. Therefore, we first compared the fluorescence signal of 6-4PPs with that of PI in individual nuclei and observed a positive linear relationship between these two values (Figure 6B). By dividing the fluorescence signal of 6-4PPs by that of PI, the relative intensity of 6-4PPs was calculated. When medians were used to draw a standard curve, good linearity between the relative intensity of 6-4PPs and UVC dose was observed (Figures 6C and 6D).

In the model experiment shown in Figure 6, we used U2OS cells, in which either endogenous *XPC* or *DDB2* gene was disrupted. Although the level of 6-4PPs was not significantly decreased in *XPC*-deficient cells during post-UV culture, the 6-4PP signals mostly disappeared within 120 min in *DDB2*

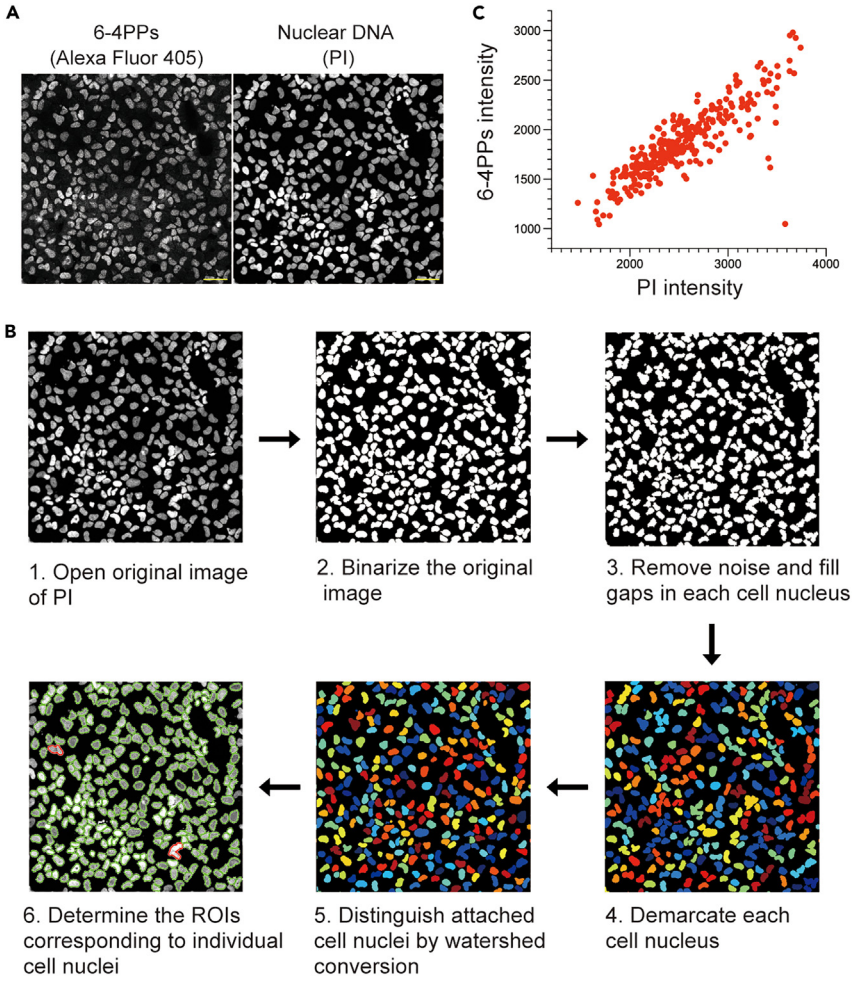

Figure 4. Measuring the fluorescence signals of 6-4PPs and DNA for individual cells with MATLAB

(A) U2OS cells were irradiated with UVC at a dose of 10 J/m^2 and fixed immediately. The cells were subjected to immunofluorescence staining with an anti-6-4PP antibody and an Alexa Fluor 405-labeled secondary antibody followed by counterstaining with PI. Representative images are shown. Scale bars: 50 μm.

(B) Schematic representation of the procedure for determining ROIs corresponding to individual cell nuclei. The image of PI fluorescence shown in (A) was used in this model analysis. The image of PI fluorescence was opened and binarized with the MATLAB code described in 49 and 50, respectively, of the section titled 'step-by-step method details' (1–2). The binarized fluorescence image was subjected to noise removal and gap filling (3: the MATLAB code is described in 51). The cell nuclei were demarcated, and attached cell nuclei were subsequently distinguished by watershed conversion (4–5: the MATLAB code is described in 52 and 53, respectively). Based on the circularity and area of each cell nucleus, remaining attached cells and signal noise were discriminated and removed with the MATLAB code described in 54–56. ROIs subjected to the following analysis are encircled with green lines, while red lines indicate removed ROIs (6).

(C) By applying the ROIs determined in (B), mean intensities per pixel of 6-4PPs and PI for individual cells were measured and presented as a two-dimensional plot.

deficient cells, in which the majority of substrate for GG-NER can be repaired except for CPD (Figure 6E). Based on these results, we concluded that this method is applicable for quantification of the relative amount of UV-induced photolesions and evaluation of GG-NER functions in cultured cells.

QUANTIFICATION AND STATISTICAL ANALYSIS

Assessing the localization of factors of interest at LUD sites

The method for quantification of relative fluorescence signals at LUD sites (F_R) is described in the section 'step-by-step method details'. The calculated F_R of each cell is used to prepare dot plots, and

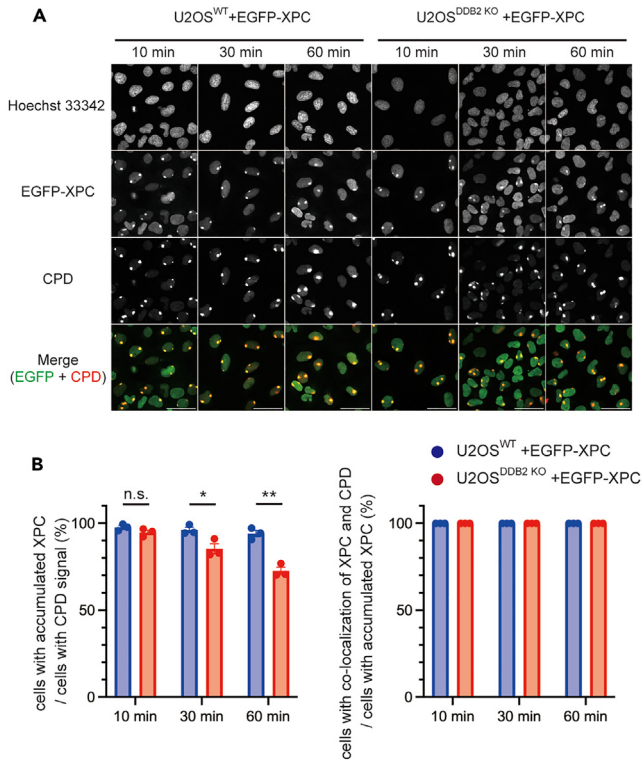

Figure 5. Assessing the accumulation of EGFP-XPC at LUD sites in the presence or absence of UV-DDB

(A) U2OS cells (wild-type or *DDB2*-deficient) stably expressing EGFP-XPC were irradiated with UVC at a dose of 400 J/m^2 through the isopore membrane filter. After incubation for the indicated time period, cells were subjected to indirect immunofluorescence staining with anti-GFP and anti-CPD antibodies and observed with a confocal laser scanning microscope. EGFP-XPC and CPDs were visualized with Alexa Fluor 488 and 594, respectively, while nuclear DNA was counterstained with Hoechst 33342. Representative images are shown. Scale bars: 50 μm.

(B) From the experiments shown in (A), the percentage of cells containing EGFP-XPC foci among cells with CPD signals was determined and shown as a bar chart (left). With the same dataset, the percentage of cells with colocalization of XPC and CPDs among cells possessing XPC foci was also calculated (right). The mean values and S.E.M. were calculated from three independent experiments. Statistical analysis was performed with the Student's t-test. *$p < 0.05$. **$p < 0.01$.

the statistical difference is assessed with parametric tests (e.g., Student's t-test for comparison of two samples and one-way ANOVA followed by Tukey's HSD tests for comparison of three or more samples) using the Prism software.

Assessing the repair kinetics of UV-induced 6-4PPs in cultured cells

After the acquisition of fluorescence images of 6-4PPs and PI, individual nuclei demarcated by PI fluorescence were set as ROIs. For each ROI, the fluorescence intensity of 6-4PPs relative to that of PI was obtained using the MATLAB code (provided above) or ImageJ macro (Supplementary information). The medians of the relative intensities of 6-4PPs obtained from individual images were used to draw a standard curve, which showed a good linear correlation between relative 6-4PP levels and UVC doses (Figure 6D). The residual 6-4PP level at each time point after UV irradiation was calculated using this standard curve, and at least three independent experiments were performed to obtain the mean values and S.E.M. The statistical difference was assessed with an appropriate parametric tests (e.g., Student's t-test for comparison of two samples and one-way ANOVA followed by Tukey's HSD tests for comparison of three or more samples) using the Prism software.

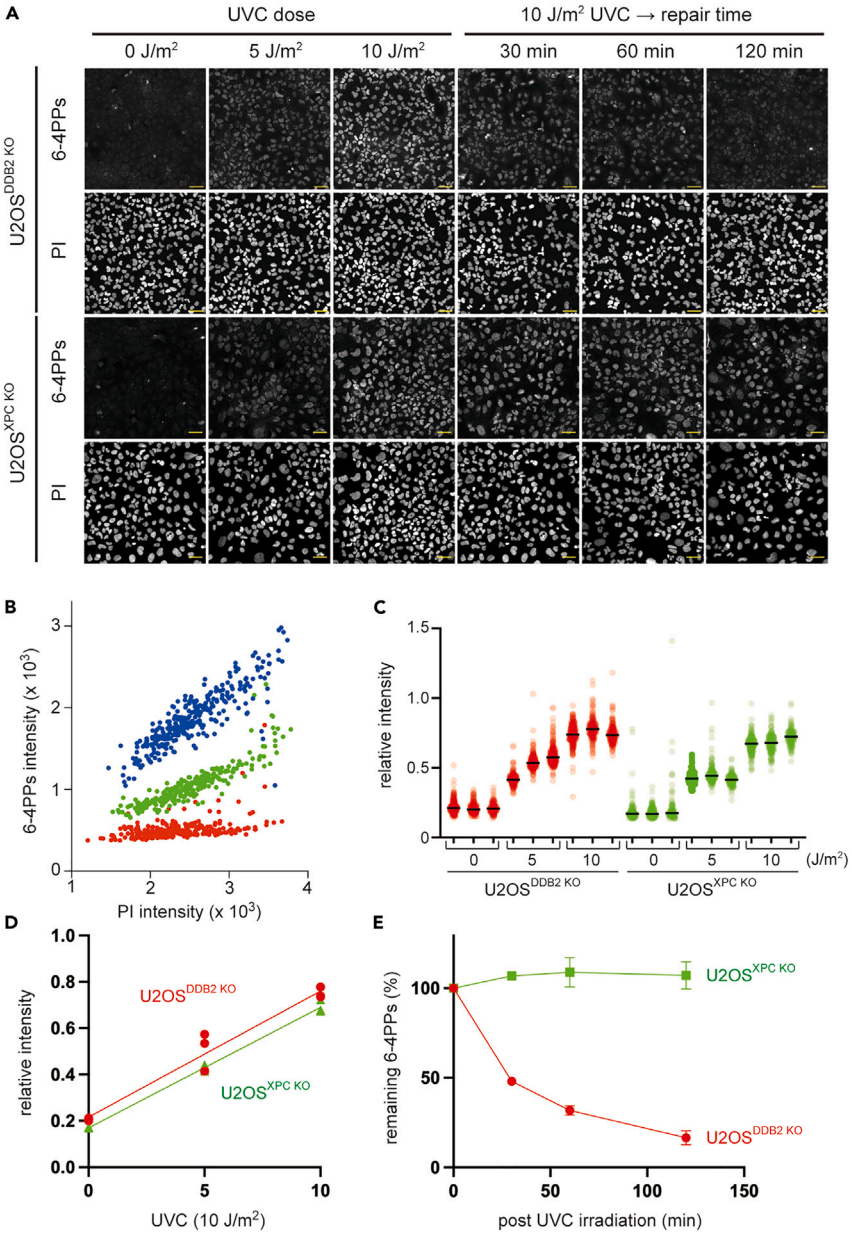

Figure 6. Assessment of repair kinetics of 6-4PPs in U2OS cells deficient and proficient in GG-NER (data were adopted from Kusakabe et al. 2022)[1]

(A) U2OS cells in which the endogenous either *DDB2* gene or *XPC* gene was disrupted (U2OS$^{DDB2\ KO}$ or U2OS$^{XPC\ KO}$, respectively) were irradiated with UVC at various doses and fixed immediately (left three columns). Furthermore, cells irradiated with UVC at a dose of 10 J/m^2 were incubated for the indicated time periods before fixation (right three columns). The cells were subjected to immunofluorescence staining with an anti-6-4PP antibody (visualized with Alexa Fluor 405) and counterstaining with PI. Representative images acquired with a confocal laser scanning fluorescence microscope are shown. Scale bars: 50 μm.

(B) Based on the images of U2OS$^{DDB2\ KO}$ cells exposed to various doses of UVC, mean fluorescence intensities of Alexa Fluor 405 (6-4PPs) and PI were quantified for individual cell nuclei by MATLAB-based method. The data of mean fluorescence intensities in each cell nucleus was used to prepare two-dimensional plot. Correlation coefficient (r) of linear approximation: 0.432 (0 J/m^2), 0.890 (5 J/m^2), 0.849 (10 J/m^2).

(C) Using each image of cells (U2OS$^{DDB2\ KO}$ and U2OS$^{XPC\ KO}$) exposed to the indicated doses of UVC, relative intensities of 6-4PPs in individual nuclei were calculated by dividing the mean fluorescence intensity of 6-4PPs by that of PI, and plotted. The black bar indicates the median of the relative intensities in each image.

Figure 6. *Continued*
(D) The medians calculated from (C) were plotted against UVC doses, which served as the standard curve for the following quantification. Correlation coefficient (r) of linear approximation: 0.982 ($U2OS^{DDB2\ KO}$), 0.998 ($U2OS^{XPC\ KO}$).
(E) From the images of cells post-UV irradiation, the medians of relative intensities of 6-4PPs were calculated using the standard curve and plotted against the recovery time. The mean values and S.E.M. were calculated from three independent experiments.

LIMITATIONS

Assessing the localization of factors of interest at LUD sites

UVC irradiation through the isopore membrane filters is an easy method to introduce DNA photolesions in local subnuclear areas and to observe altered localization of various factors. With this method, however, it is not possible to control which cell or which part of a cell nucleus is exposed to UV. In addition, it is difficult to assess UV-induced relocalization of factors at very early time points due to a time lag between conventional UV irradiation and the start of microscopic observation. One solution to these problems is to use a specialized confocal laser microscope equipped with a femtosecond pulse laser or a UVC laser.[9] Our recent studies utilized a 780 nm fs laser and three-photon absorption, to induce DNA photolesions at any site of interest and assess the kinetics of protein recruitment in real time.[1]

In addition, the usefulness and reliability of the immunofluorescence-based assays described here strongly depend on the characteristics of the antibodies used, such as their specificity, affinity, and epitope position in the target molecule. If no appropriate antibody is available, expression of fluorescently labeled target proteins is another option. In our recent paper, we showed the recruitment of MTA proteins, activators of HDAC1/2, to LUD sites[1] using MTAs fused to HaloTag 7 and transiently expressed in cells.

Assessing the repair kinetics of UV-induced 6-4PPs in cultured cells

Although this method is useful for quantitative assessment of overall DNA repair rates *in vivo*, it does not provide information about repair kinetics at specific genomic loci. If necessary, other experiments, such as a T4 endonuclease V-based assay or next-generation sequencing-based assays, such as repair-seq,[20–22] could be considered.

TROUBLESHOOTING

Problem 1

Many cells are detached after removing polycarbonate isopore membrane filters (step-by-step method details 3-a).

Potential solution

This problem may be caused by overly tight adhesion of the filter to the cells. Before covering cells with a filter, it is recommended not to remove PBS thoroughly but to leave a small amount (approximately 10 μL per 14 mm glass bottom hole) at the edge of the glass bottom hole.

Problem 2

The accumulation of XPC at LUD sites is obscure (step-by-step method details 3-a).

Potential solution

The cause of this problem could be that too much PBS remains in the glass bottom hole before placement of the isopore membrane filter. The thin layer of remaining PBS between the filter and cells absorbs UVC and causes the filter to drift during irradiation. Because thorough removal of PBS causes another problem (see problem 1), it is particularly important to leave an appropriate amount of PBS in the glass bottom hole, which may need to be determined empirically.

Problem 3

Recruitment or dissociation of factors of interest is unclear or not observed (step-by-step method details 4–18).

Potential solution

First of all, it should be kept in mind that the localization of the factors may not change upon local UV irradiation. However, another possibility is that the antibody used is not suitable for immunofluorescence staining. To validate the reliability of the antibodies, it is important to check whether immunofluorescence signals are decreased after depletion of the target proteins. If no antibody is available for immunofluorescence staining, expression of the protein fused to an appropriate tag is one solution. In any case, protein accumulation can be difficult to discern if only a small fraction of the protein is recruited to LUD sites. If any tagged protein is ectopically expressed, it is better to avoid overexpression. Moreover, as described in the section 'step-by-step method details' (3-b), relatively weak accumulation of some target proteins may become more discernable by performing pre-extraction, which removes the fraction of proteins not tightly associated with chromatin and thereby reduces background signals. One of such examples was shown with proliferating cell nuclear antigen (PCNA).[16]

Problem 4

The number of cells is decreased after UVC irradiation and immunofluorescence staining (step-by-step method details 30–31).

Potential solution

In general, these experiments are easier if the adhesion of cells to culture vessels is tighter (U2OS is a relatively good cell line for this purpose). Depending on the characteristics of cell lines used, appropriate treatment of glass bottom surfaces may be required. For instance, poly-D-lysine coated 96-well glass bottom plates are commercially available (e.g., GP96001, Matsunami Glass Industry). An alternative is trying other assays, such as an enzyme-linked immunosorbent assay.[12]

Problem 5

Fluorescence signals of 6-4PPs vary depending on positions in the same well (step-by-step method details 47).

Potential solution

One possibility is that a small amount of medium remained in the well, particularly at the edge of the bottom, during UVC irradiation. Make sure to remove as much solution as possible from the well with a pipette or an aspirator. The distance between germicidal lamps and sample plates is also critical. We set lamps at ~1.5 m in height from samples so that UV radiation comes down almost vertically. This prevents the wall of a well from shading the bottom surface and also minimizes variations in UV fluence among wells at different positions. Moreover, it is also crucial to use a sufficient volume of antibody solutions to cover the entire bottom surface of wells/dishes. Particularly, it should be noted that the cells near the center of wells tends to be covered more shallowly and even dried out due to the effect of meniscus. With 96-well plates, we use 50 μL antibody solution per well, while the appropriate volume should be determined if dishes of different size are used.

RESOURCE AVAILABILITY

Lead contact

Further information and requests for resources and reagents should be directed to and will be fulfilled by the lead contact, Kaoru Sugasawa (ksugasawa@garnet.kobe-u.ac.jp).

Materials availability

The U2OS cell lines and the plasmids used in this work are available from the corresponding author upon request.

Data and code availability

The datasets of fluorescence images used for image analyses were deposited to Mendeley Data (https://doi.org/10.17632/5btczp897z.1). The MATLAB code and the Fiji/ImageJ code used for analysis were provided in this paper.

SUPPLEMENTAL INFORMATION

Supplemental information can be found online at https://doi.org/10.1016/j.xpro.2023.102378.

ACKNOWLEDGMENTS

The illustration of a confocal laser microscope in the graphical abstract was adopted from the Togo Picture Gallery (https://togotv.dbcls.jp/pics.html). This work was supported by grants-in-aid (KAKENHI) to K.S. (grant numbers JP16H06307 and JP21H03598) and M.K. (grant number JP21K17889).

AUTHOR CONTRIBUTIONS

M.K. and K.S. designed the experiments and wrote the manuscript. M.K. validated and performed the experiments.

DECLARATION OF INTERESTS

The authors declare no competing interests.

REFERENCES

1. Kusakabe, M., Kakumu, E., Kurihara, F., Tsuchida, K., Maeda, T., Tada, H., Kusao, K., Kato, A., Yasuda, T., Matsuda, T., et al. (2022). Histone deacetylation regulates nucleotide excision repair through an interaction with the XPC protein. iScience *25*, 104040. https://doi.org/10.1016/j.isci.2022.104040.

2. Schärer, O.D. (2013). Nucleotide excision repair in eukaryotes. Cold Spring Harb. Perspect. Biol. *5*, a012609. https://doi.org/10.1101/cshperspect.a012609.

3. Sugasawa, K., Ng, J.M., Masutani, C., Iwai, S., van der Spek, P.J., Eker, A.P., Hanaoka, F., Bootsma, D., and Hoeijmakers, J.H. (1998). Xeroderma pigmentosum group C protein complex is the initiator of global genome nucleotide excision repair. Mol. Cell *2*, 223–232. https://doi.org/10.1016/s1097-2765(00)80132-x.

4. Volker, M., Moné, M.J., Karmakar, P., van Hoffen, A., Schul, W., Vermeulen, W., Hoeijmakers, J.H., van Driel, R., van Zeeland, A.A., and Mullenders, L.H. (2001). Sequential assembly of the nucleotide excision repair factors in vivo. Mol. Cell *8*, 213–224. https://doi.org/10.1016/s1097-2765(01)00281-7.

5. van Toorn, M., Turkyilmaz, Y., Han, S., Zhou, D., Kim, H.-S., Salas-Armenteros, I., Kim, M., Akita, M., Wienholz, F., Raams, A., et al. (2022). Active DNA damage eviction by HLTF stimulates nucleotide excision repair. Mol. Cell *82*, 1343–1358.e8. https://doi.org/10.1016/j.molcel.2022.02.020.

6. Adam, S., Polo, S.E., and Almouzni, G. (2013). Transcription recovery after DNA damage requires chromatin priming by the H3.3 histone chaperone HIRA. Cell *155*, 94–106. https://doi.org/10.1016/j.cell.2013.08.029.

7. Piquet, S., Le Parc, F., Bai, S.-K., Chevallier, O., Adam, S., and Polo, S.E. (2018). The histone chaperone FACT coordinates H2A.X-dependent signaling and repair of DNA damage. Mol. Cell *72*, 888–901.e7. https://doi.org/10.1016/j.molcel.2018.09.010.

8. Kakumu, E., Nakanishi, S., Shiratori, H.M., Kato, A., Kobayashi, W., Machida, S., Yasuda, T., Adachi, N., Saito, N., Ikura, T., et al. (2017). Xeroderma pigmentosum group C protein interacts with histones: regulation by acetylated states of histone H3. Gene Cell. *22*, 310–327. https://doi.org/10.1111/gtc.12479.

9. Dinant, C., de Jager, M., Essers, J., van Cappellen, W.A., Kanaar, R., Houtsmuller, A.B., and Vermeulen, W. (2007). Activation of multiple DNA repair pathways by sub-nuclear damage induction methods. J. Cell Sci. *120*, 2731–2740. https://doi.org/10.1242/jcs.004523.

10. Kusakabe, M., Onishi, Y., Tada, H., Kurihara, F., Kusao, K., Furukawa, M., Iwai, S., Yokoi, M., Sakai, W., and Sugasawa, K. (2019). Mechanism and regulation of DNA damage recognition in nucleotide excision repair. Genes Environ. *41*, 2. https://doi.org/10.1186/s41021-019-0119-6.

11. Ory, D.S., Neugeboren, B.A., and Mulligan, R.C. (1996). A stable human-derived packaging cell line for production of high titer retrovirus/vesicular stomatitis virus G pseudotypes. Proc. Natl. Acad. Sci. USA *93*, 11400–11406. https://doi.org/10.1073/pnas.93.21.11400.

12. Akita, M., Tak, Y.-S., Shimura, T., Matsumoto, S., Okuda-Shimizu, Y., Shimizu, Y., Nishi, R., Saitoh, H., Iwai, S., Mori, T., et al. (2015). SUMOylation of xeroderma pigmentosum group C protein regulates DNA damage recognition during nucleotide excision repair. Sci. Rep. *5*, 10984. https://doi.org/10.1038/srep10984.

13. Sakai, W., Yuasa-Sunagawa, M., Kusakabe, M., Kishimoto, A., Matsui, T., Kaneko, Y., Akagi, J.-I., Huyghe, N., Ikura, M., Ikura, T., et al. (2020). Functional impacts of the ubiquitin-proteasome system on DNA damage recognition in global genome nucleotide excision repair. Sci. Rep. *10*, 19704. https://doi.org/10.1038/s41598-020-76898-2.

14. Schindelin, J., Arganda-Carreras, I., Frise, E., Kaynig, V., Longair, M., Pietzsch, T., Preibisch, S., Rueden, C., Saalfeld, S., Schmid, B., et al. (2012). Fiji: an open-source platform for biological-image analysis. Nat. Methods *9*, 676–682. https://doi.org/10.1038/nmeth.2019.

15. van der Meer, P.J., Van Den Heuvel, D., and Luijsterburg, M.S. (2023). Unscheduled DNA synthesis at sites of local UV-induced DNA damage to quantify global genome nucleotide excision repair activity in human cells. Bio. Protoc. *13*, e4609. https://doi.org/10.21769/BioProtoc.4609.

16. Katsumi, S., Kobayashi, N., Imoto, K., Nakagawa, A., Yamashina, Y., Muramatsu, T.,

Shirai, T., Miyagawa, S., Sugiura, S., Hanaoka, F., et al. (2001). In situ visualization of ultraviolet-light-induced DNA damage repair in locally irradiated human fibroblasts. J. Invest. Dermatol. *117*, 1156–1161. https://doi.org/10.1046/j.0022-202x.2001.01540.x.

17. Kimura, H., Hayashi-Takanaka, Y., Goto, Y., Takizawa, N., and Nozaki, N. (2008). The organization of histone H3 modifications as revealed by a panel of specific monoclonal antibodies. Cell Struct. Funct. *33*, 61–73. https://doi.org/10.1247/csf.07035.

18. Stirling, D.R., Swain-Bowden, M.J., Lucas, A.M., Carpenter, A.E., Cimini, B.A., and Goodman, A. (2021). CellProfiler 4: improvements in speed, utility and usability. BMC Bioinf. *22*, 433. https://doi.org/10.1186/s12859-021-04344-9.

19. Nakagawa, A., Kobayashi, N., Muramatsu, T., Yamashina, Y., Shirai, T., Hashimoto, M.W., Ikenaga, M., and Mori, T. (1998). Three-dimensional visualization of ultraviolet-induced DNA damage and its repair in human cell nuclei. J. Invest. Dermatol. *110*, 143–148. https://doi.org/10.1046/j.1523-1747.1998.00100.x.

20. Hanawalt, P.C. (1989). Preferential repair of damage in actively transcribed DNA sequences in vivo. Genome *31*, 605–611. https://doi.org/10.1139/g89-113.

21. Hu, J., Adebali, O., Adar, S., and Sancar, A. (2017). Dynamic maps of UV damage formation and repair for the human genome. Proc. Natl. Acad. Sci. USA *114*, 6758–6763. https://doi.org/10.1073/pnas.1706522114.

22. Hu, J., Adar, S., Selby, C.P., Lieb, J.D., and Sancar, A. (2015). Genome-wide analysis of human global and transcription-coupled excision repair of UV damage at single-nucleotide resolution. Genes Dev. *29*, 948–960. https://doi.org/10.1101/gad.261271.115.